Plant Disease • 2026 • 110:890-902 • https://doi.org/10.1094/PDIS-01-25-0126-RE

The 2022 Fusarium Head Blight Outbreak in Ethiopia: Emerging Pathogens, Mixed Mycotoxins, and Interspecies Interactions

Liza M. DeGenring,[1] Ashenafi Gemechu,[2] Vahideh Rafiei,[3] Karen Broz,[1] Gizachew H. Regasa,[2] Kiara Munsamy,[4] Neriman Yilmaz,[4] Yanhong Dong,[5] Matthew N. Rouse,[6] and Milton T. Drott[1,†]

[1] United States Department of Agriculture, Agriculture Research Service, Cereal Disease Lab, St. Paul, MN, U.S.A.
[2] Ethiopian Institute of Agricultural Research, Addis Ababa, Ethiopia
[3] Department of Forest Mycology and Plant Pathology, Swedish University of Agricultural Sciences, Uppsala, Sweden
[4] Forestry and Agricultural Biotechnology Institute, University of Pretoria, Pretoria, South Africa
[5] Department of Plant Pathology, University of Minnesota, St. Paul, MN, U.S.A.
[6] United States Department of Agriculture, Agricultural Research Service, Sugarcane Field Station, Canal Point, FL, U.S.A.

Abstract

As Ethiopia pushes toward self-sufficiency in wheat production, it has escaped large outbreaks of Fusarium head blight (FHB), a disease that threatens wheat production globally. However, in 2022, FHB incidences in Ethiopia rose to 80%, with some areas experiencing 100% disease severity. Here we provide insights into the etiology of this disease outbreak and point toward future directions to mitigate the emerging threat of FHB on a global scale. Although most wheat samples from 2022 exhibited low trichothecene levels, 26% exceeded recommended thresholds and several contained multiple trichothecene variants. We obtained 64 isolates from the outbreak and identified diverse members of the *Fusarium graminearum* species complex (FGSC) and many *Epicoccum* species. The FGSC species contributing to the outbreak are rare on a global scale. Genomic analyses reveal that *Fusarium aethiopicum* has persisted in Ethiopia for decades and shares ancient ancestry with a newly emerged novel species in the FGSC that we formally described as *Fusarium kistleri*. Single-nucleotide polymorphism–based analyses suggest high clonal fraction among FGSC isolates in Ethiopia, raising questions about a recent population expansion. Our findings reveal that although *Epicoccum* alone causes minimal disease on wheat, its presence can have a small but synergistic impact on disease symptoms when *F. graminearum* has already infected. The unique diversity and species composition of the 2022 Ethiopian outbreak underscores the importance of addressing emerging threats in a globalized agricultural economy to secure food safety, food security, and global food equity.

Keywords: deoxynivalenol, Ethiopia, *Fusarium graminearum*, global food security, trichothecenes

Wheat is a staple food crop worldwide, with global production exceeding 800 million tons in 2022 (Food and Agriculture Organization of the United Nations 2021), providing 20% of daily calories and protein (Shiferaw et al. 2013). Ethiopia is the second largest producer of wheat in Africa behind Egypt, producing 5.2 million tons in 2022 (Food and Agriculture Organization of the United Nations 2021). The Ethiopian government and international organizations have supported efforts to increase wheat production, aiming to transition Ethiopia from a wheat importer to a self-sufficient producer and exporter; this initiative has included at least $94 million in international financial support (Reidy 2024). Bread wheat (*Triticum aestivum* L.) and durum wheat (*Triticum turgidum* var. *durum*) are the main species grown in Ethiopia. Cultivation is typically relegated to the highland regions in Oromia and Amhara at elevations ranging from 1,600 to 3,500 m above sea level (Anteneh and Asrat 2020) and is dominated by smallholder farmers (Demeke and Di Marcantonia 2013; Minot et al. 2015). In addition to providing food security as a staple food crop in Ethiopia, wheat production provides a livelihood for millions of smallholder farmers and laborers, contributing significantly to the country's gross domestic product (Amentae et al. 2017; Minot et al. 2015; Negassa et al. 2013). Although work has been done to improve wheat yields in Ethiopia, there are still major barriers to reaching the goal of self-sufficiency including infrastructure, agricultural practices, and diseases (Anteneh and Asrat 2020; Tadesse et al. 2019).

Fusarium head blight (FHB) is one of the most important diseases of wheat and other cereal crops worldwide (Alisaac and Mahlein 2023; Schmale and Bergstrom 2003), leading to billions of dollars in losses globally (McMullen et al. 2012). FHB is predominantly caused by species in the *Fusarium graminearum* species complex (FGSC) (O'Donnell et al. 2004). *Fusarium graminearum* Schwabe is the species most commonly associated with FHB (Goswami and Kistler 2004; O'Donnell et al. 2000; Starkey et al. 2007; Xu et al. 2022). In addition to yield reductions, cereals with FHB are contaminated with mycotoxins, most notoriously, trichothecenes, that threaten human and animal health (Desjardins 2006). The FGSC exhibits a diversity of trichothecene chemotypes, with different isolates producing nivalenol (NIV) (Gale et al. 2011),

[†]Corresponding author: M. T. Drott; Milton.Drott@usda.gov

L. M. DeGenring and A. Gemechu contributed equally to this work.

Data availability: The genome sequences generated in this study have been deposited in the NCBI GenBank database under BioProject accession number PRJNA1255107 upon publication of the manuscript. Individual genome assemblies are accessible using GenBank accession numbers (Supplementary Table S7). Raw sequencing reads will be available in the Sequenced Read Archive (SRA) under the same BioProject with accession numbers SAMN48283755 to SAMN48283765. The internal transcribed spacer (ITS) sequences generated in this study have been deposited in the NCBI GenBank database under accession number PV801520 to PV801582.

Disclaimer: Mention of trade names or commercial products in this publication is solely for purpose of providing specific information and does not imply recommendation or endorsement by the United States Department of Agriculture (USDA). USDA is an equal opportunity provider and employer.

Funding: Support was provided by the United States Department of Agriculture-Agricultural Research Service Project 5062-21220-024-000D to M. T. Drott and through a competitive Participating Agency Service Agreement awarded to M. T. Drott.

***e*-Xtra:** Supplementary material is available online.

The author(s) declare no conflict of interest.

Accepted for publication 26 June 2025.

15-acetyl-deoxynivalenol (15ADON), 3-acetyl-deoxynivalenol (3ADON) (Goswami and Kistler 2004; Ward et al. 2002), or NX-2 (Varga et al. 2015). Both acetylated derivatives of deoxynivalenol (15ADON and 3ADON) are converted to DON through deacetylation during plant infection, contributing to overall DON toxicity (Schmeitzl et al. 2015). Research suggests that chemotype is associated with host range, fitness traits, and toxin accumulation in the host (Gale et al. 2011; Kelly and Ward 2018). Additionally, the virulence of the FHB pathogen can be directly related to the level of trichothecene produced in the plant (Hao et al. 2023; Jansen et al. 2005). Many countries have established regulations for permissible levels of these mycotoxins in both processed and unprocessed foods (Haile et al. 2019). However, not all countries have developed mycotoxin detection networks, leaving nations vulnerable to export rejections and contamination risks in staple food sources (Ayelign and De Saeger 2020).

Over the last decades, FHB outbreaks have increased globally because of changes in agricultural practices, such as reduced tillage, use of susceptible wheat varieties, and intensification of wheat production, as well as the impact of environmental instability (Alisaac and Mahlein 2023). Ethiopia's push toward wheat self-sufficiency has not been spared this scourge. Indeed, upon discovery of a new FGSC specie in Ethiopia, *Fusarium aethiopicum*, O'Donnell et al. (2008) suggested that the majority of species within FGSC have evolutionary origins in the Southern Hemisphere. Although *F. aethiopicum* poses a potential threat to African wheat, global research has prioritized species that are more common in other regions (Amarasinghe et al. 2019; Del Ponte et al. 2022; Laraba et al. 2023; McMullen et al. 2012), leaving a globalized agroeconomy vulnerable to emerging FHB pathogens. FHB has not historically posed a significant threat in Ethiopia; instead, the large impact of rust diseases has been the focus of the country's research (Allen-Sader et al. 2019; Nigus et al. 2022; Tadesse et al. 2022). However, in recent years, reports of FHB outbreaks have increased in Ethiopia, with prevalence reaching up to 90% in wheat fields surveyed (Kebede et al. 2021) and the disease reaching epidemic levels in 2022. The lack of historical data on this emerging threat has prompted Ethiopian farmers to seek guidance on controlling FHB in their fields (A. Gemechu, *personal observation*).

Many of the current FHB management practices have been developed in the United States and Europe, leaving questions about what approaches will translate to African growing environments. Although FHB resistance in wheat lines can be helpful for disease management (Getahun et al. 2024), it is unclear which cultivars would be most resistant in Ethiopia. Addressing the threat of FHB that emerged in 2022 has been challenging owing to limited knowledge about the outbreak's etiology. In this study, we sought to clarify the etiology of the 2022 FHB outbreak in Ethiopia to provide a foundation for disease management decisions in the future. Additionally, we describe a novel *Fusarium* specie isolated from wheat in Ethiopia based on morphological and phylogenetic distinctions. The specific objectives of this study were to (i) identify the causal pathogens associated with FHB symptoms on wheat; (ii) quantify trichothecene contamination of wheat flour; (iii) determine trichothecene chemotype of FGSC isolates; and (iv) determine the genetic relationship of the Ethiopian FGSC isolates compared with public data.

Materials and Methods

Fungal isolates

Symptomatic wheat samples were collected from randomly selected fields in the Oromia (East Shewa Zone) and Amhara (North Shewa Zone) regions of Ethiopia in 2022 (Fig. 1). The samples were collected from 10 to 15 wheat heads per field exhibiting typical symptoms of FHB. Three to five symptomatic kernels from each head were surface sterilized in a 5% sodium hypochlorite solution for 3 min and rinsed three times in distilled water for 3 min. Kernels were placed on potato dextrose agar (PDA). After 7 to 10 days, a total of 64 isolates were purified by single-spore isolation. Plugs of the resulting colonies were preserved as 50% glycerol stocks at −80°C. To obtain wheat flour for trichothecene quantification, the remaining wheat heads were threshed and winnowed manually. Grain samples of 50 g were ground using a sample grinder and prepared for trichothecene evaluation as described below.

Fungal DNA extraction and PCR amplification

To obtain DNA for PCR amplification, all 64 isolates were grown in complete medium (Correll et al. 1987) for 4 days at 25°C, washed with sterile water, frozen at −80°C, and lyophilized. DNA was extracted as described in Drott et al. (2019) with minor modifications. Briefly, lyophilized tissue was disrupted for 45 s using a Mini-Beadbeater-8 Cell Disrupter (BioSpec Products, Bartlesville, OK, U.S.A.) set on Homogenize and centrifuged for 30 s at full speed (21,300 rcf), and 750 µl extraction buffer was added. Samples were then vortexed for 20 s, incubated for 10 min in a 95°C Fisherbrand Isotemp FS Drybath heat block (Fisher Scientific, Emeryville, CA, U.S.A.), and then centrifuged for 15 min at 16,000 rcf. The supernatant (approximately 500 µl) was then transferred to a new tube. DNA was diluted 1:4 in nuclease-free water for use as template for PCR.

Fungal ITS region was amplified using primers ITS1F 5′- TCC GTAGGTGAACCTGCGG-3′ and ITS4 5′-TCCTCCGCTTAT TGATATGC-3′ (White et al. 1990). PCR amplification was performed in 20-µl reactions with 0.5 units of TAKARA ExTaq (Takara Bio U.S.A., San Jose, CA, U.S.A.), 1× TAKARA ExTaq buffer, 1 µM of each primer, 0.2 mM of TAKARA dNTPs (2.5 mM each dNTP), 1 µl of DNA template, and nuclease-free water to 20 µl. DNA amplification was conducted in an Bio-Rad DNA Engine thermocycler (Bio-Rad Laboratories, Hercules, CA, U.S.A.) with the following program: initial denaturing of one cycle of 94°C for 2 min, followed by 29 cycles of denaturing at 94°C for 1 min, annealing at 55°C for 1 min, extension at 72°C for 1 min, a final extension at 72°C for 10 min, and holding at 10°C. The PCR product (5 µl) of each sample was run on a 1% agarose gel (Seakem LE, Lonza, Basel, Switzerland) with 0.5× Tris-Borate-EDTA (TBE) buffer for gel electrophoresis. Single amplicons of approximately 600 bp were observed. The remaining PCR product (15 µl) of each sample was cleaned with ExoSAP-IT PCR Product Cleanup (Thermo Fisher Scientific, Waltham, MA, U.S.A.) as per Lofgren et al. (2018). Cleaned samples were Sanger sequenced using primer ITS1F and ITS4, each in individual reactions, at Azenta Life Sciences GENEWIZ (South Plainfield, NJ, U.S.A.). Sequences were trimmed using Benchling (https://www.benchling.com/). If both primer sequencing reactions for an isolate were successful, consensus sequence was generated using Benchling. Preliminary species assignment was obtained using ITS sequences in a BLASTN (version BLASTN 2.13.0+) search of the core nucleotide database on the NCBI BLAST website (Zhang et al. 2000). To confirm species identifications, we downloaded all publicly available ITS sequences of Sordariomycetes from NCBI on 13 April 2023. The resulting dataset was combined with our sequence data and aligned using MAFFT (v. 7.475) with the "auto" parameter. Resulting alignments were trimmed with trimAl (v. 1.4.rev15) (Capella-Gutiérrez et al. 2009) using the "automated1" parameter and constructed into phylogenies with IQtree2 (v. 2.1.2) (Minh et al. 2020) using 1,000 ultrafast bootstraps and model selection via the "test" parameter.

Trichothecene chemotype

The trichothecene chemotype for all isolates identified as part of the FGSC was inferred from genotypic data using 15-*O*-acetyltransferase (Tri3) and trichothecene efflux pump (Tri12) multiplex PCR (Starkey et al. 2007; Ward et al. 2002) and Tri1 PCR-RFLP (Liang et al. 2014). Tri3 and Tri12 multiplex PCR amplification were performed in 10-µl reactions with 0.25 units of TAKARA ExTaq, 1× TAKARA ExTaq buffer, 0.2 µM of each primer, 0.2 mM of TAKARA dNTPs (2.5 mM each dNTP), 2 µl of DNA template, and nuclease-free water to 10 µl. PCR amplification was conducted in a Bio-Rad DNA Engine thermocycler (Bio-Rad Laboratories) with the following program: initial denaturing of one cycle of 94°C for

2 min, followed by 25 cycles of denaturing at 94°C for 30 s, annealing at 52°C for 30 s, extension at 72°C 1 min, a final extension at 72°C for 10 min, and holding at 10°C. The PCR product (5 µl) of each sample was run on a 1.5% agarose 0.5× TBE gel. Amplicon sizes for trichothecene chemotypes with Tri3 multiplex primers were 840 bp for nivalenol; 610 bp for 15-acetyldeoxynivalenol; and 243 bp for 3-acetyldeoxynivalenol. Amplicon sizes for trichothecene chemotypes with Tri12 multiplex primers: 840 bp for nivalenol; 670 bp for 15-acetyldeoxynivalenol; and 410 bp for 3-acetyldeoxynivalenol.

Tri1 PCR-RFLP PCR reactions used to identify potential NX-2 producers were performed in 20-µl reactions as described above for ITS primers, but with 2 µl of DNA template. The run was conducted in a Bio-Rad DNA Engine thermocycler (Bio-Rad Laboratories) using the following cycling conditions: initial denaturing of one cycle of 94°C for 2 min, followed by 25 cycles of denaturing at 94°C for 30 s, annealing at 50.3°C for 1 min, extension at 72°C for 105 s, a final extension at 72°C for 10 min, and holding for 10°C. The PCR product (5 µl) of each sample was run on a 1% agarose 0.5× TBE gel. Remaining sample was digested with ApoI (NEB, Ipswich, MA, U.S.A.) in 20-µl reactions with 1× NEB buffer 3.1, 5 units of ApoI, and 3.5 µl of water. Digests were incubated for 2 h at 50°C and run on a 1.5% agarose 0.5× TBE gel. Fragment sizes following digestion for trichothecene chemotypes were as follows: 888- and 851-bp fragments for nivalenol, 15-acetyldeoxynivalenol, and 3-acetyldeoxynivalenol; 407-, 482-, and 851-bp fragments for NX-2.

DNA extractions for whole-genome sequencing

All 12 isolates (Supplementary Table S1) determined to be part of FGSC were selected for whole-genome sequencing. To extract their DNA, the isolates were grown in complete medium (Correll et al. 1987) for 4 days at 25°C, washed with sterile water, frozen at −80°C, and lyophilized. Tissue was homogenized in a microcentrifuge tube containing 0.25 g of 0.5-mm soda-lime glass beads (BioSpec Products) for 3 s. DNA was extracted from the disrupted tissue as described in (Drott et al. 2020) with slight modifications. Briefly, the tissue was dissolved in 700 µl of LETS buffer. The resulting suspension was purified by the addition of an equal volume of phenol: chloroform: isoamyl alcohol (25:24:1) and centrifuging the tubes at 15,060 rpm for 10 min at 4°C. This purification was repeated twice, with 100 µl less volume each time. Genomic DNA was precipitated by adding 1 ml of cold 95% ethanol and pelleted by centrifuging at 15,060 rpm for 10 min at 4°C. The pelleted DNA was washed with 70% ethanol, air dried, dissolved in 40 µl of 10-mM Tris buffer (pH 8) and 1 µl of RNAse A (10 mg/ml), and then incubated at 50°C for 30 min. The DNA was stored at −20°C until sequenced.

Whole-genome sequencing

Whole-genome sequencing for six of the isolates (Supplementary Table S1) was performed on an Oxford Nanopore MinION Mk1B platform using the Native Barcoding Kit 24 (version 14; SQK-RBK114-24) and a FLO-MIN114 flow cell over a 72-h run time (Oxford Nanopore Technologies, Oxford, U.K.). Dorado (version 0.5.0) basecalling software was used to obtain duplex reads and

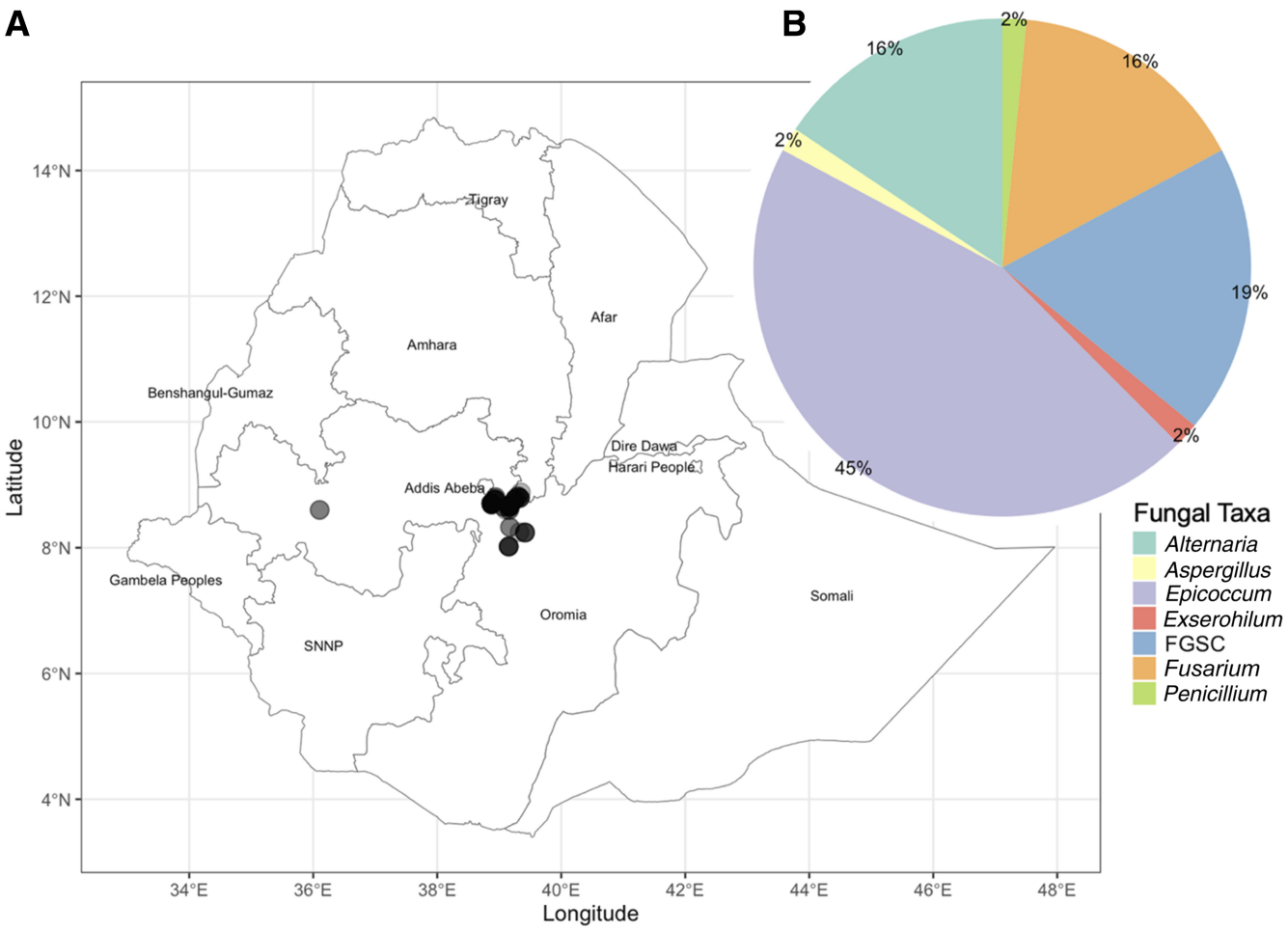

Fig. 1. The distribution of sampling locations across Ethiopia and the species identity of resulting isolates. **A,** A map of Ethiopia where darker dots represent an overlapping of the 25 total collection locations. Major geographic regions are labeled with the Southern Nations, Nationalities, and Peoples' Region abbreviated to SNNP. **B,** A pie chart depicting the fungal taxa identification of 64 isolates collected from Ethiopia in 2022. Taxa were confirmed through BLASTN of internal transcribed spacer sequences. Whereas most taxa are identified at the genus level, the *Fusarium graminearum* species complex (FGSC), a subset of the *Fusarium* genus, is presented separately to emphasize the species that are the focus of this study. Identifications below the genus level were based on phylogenetic analyses depicted in Supplementary Figure S3.

a binary alignment/map (BAM) file for each isolate. We discarded the sequences with a minimum quality read score of less than 10 or a read length of less than 200 bp. The resulting BAM files were converted to FASTQ files using SAMtools (v. 1.9) (Li et al. 2009). Genomes were assembled with Flye (v. 2.9.4) (Kolmogorov et al. 2019) using nanopore hq parameters. QUAST (v. 4.3) (Gurevich et al. 2013) was run against the NCBI reference genome assembly of *F. graminearum* PH-1 (GCA_000240135.3) to determine genome quality. The completeness of assemblies was assessed with BUSCO (Benchmarking Universal Single-Copy Orthologs) (v. 5.4.7) using the sordariomycetes_odb10 databases (Simão et al. 2015) (QUAST and BUSCO outputs are reported in Supplementary Table S2).

Whole-genome sequencing for eight of the isolates, including two sequenced with Nanopore (Supplementary Table S1), was performed on an Illumina Nova Seq 6000 Platform (paired-end 150-bp reads; PE150) at Novogene (Sacramento, CA). Library preparation was conducted using the Rapid Plus DNA Library Prep Kit (RK20208). Low-quality reads (Qscore ≤5; N > 10%) and adapters were removed by the company. Prior to assembly, raw reads were quality controlled using the *bbduk.sh* script from BBMap (v. 39.01) (Bushnell 2014). Genomes were de novo assembled with SPAdes (v. 3.10.0) (Bankevich et al. 2012). QUAST and BUSCO were run on assembled genomes as previously described (Supplementary Table S2). For two of the isolates that had both long-read and short-read data (Supplementary Table S1), a de novo hybrid assembly was constructed using SPAdes.

Three maximum likelihood trees were constructed to confirm the relationship between the Ethiopian species and publicly available sequence data. First, data from Laraba et al. (2021) were used to create a maximum likelihood tree using three housekeeping genes, RNA polymerase II largest subunit (RPB1), RNA polymerase II second largest subunit (RPB2), and translation elongation factor (TEF1). Second, data from O'Donnell et al. (2008) were used to create a maximum likelihood tree using five housekeeping genes, TEF1, histone H3, internal transcribed spaces 28S ribosomal RNA (ITS28S), alpha-tubulin (atub), and reductase gene (rg), as these were the only genes that we were able to reliably find the data for across all relevant isolates from the past citations. For these two trees, sequences from the studies were used as BLASTN queries in the BLAST + suite (v. 2.16.0). The top hit from each query was extracted from the target genome using bedtools getfasta (v. 2.31.1) (Quinlan and Hall 2010). Although concatenation within gene sequences from O'Donnell et al. (2008) was too laborious (or cryptic) to incorporate into our study (resulting in an inability to incorporate affected genes), the RPB2 sequence from Laraba et al. (2021) resulted in two hits that were concatenated. The resulting sequences for each gene were aligned with the respective data from each study aligned using MAFFT (v. 7.475) with the "auto" parameter and trimmed with TrimAl (v. 1.4.rev15) using the "automated1" parameter. Resulting trimmed alignments were used to construct a maximum likelihood tree using a partition model in IQtree2 (v. 2.1.2) with the model "test" parameter and 1,000 ultrafast bootstraps.

Finally, we downloaded 79 publicly available genomes of FGSC isolates from NCBI (Supplementary Table S3) and combined these data with our assembled genomes. Genomes were scanned for BUSCOs (v. 5.4.7) using the sordariomycetes_odb10 dataset. A subset of 2,580 BUSCOs that were present in all isolates were individually aligned, trimmed, and used to construct a tree with methods identical to those used for the other two trees above. All three trees were imported into R using "ape" package and visualized using tools from "treeio" and "ggtree."

To contextualize the data from the 12 FGSC isolates from Ethiopia, raw reads from Kulik et al. (2022) and Kelly and Ward (2018) were downloaded from NCBI. Short reads were aligned to the PH-1 reference (GCA_000240135.3) using BWA mem (Li 2013), whereas long reads were aligned using minimap2 using parameters for nanopore sequence data (Li 2018). Variants were called using the Genome Analysis Toolkit (GATK v. 4.0.12.0) (Van der Auwera and O'Connor 2020) using parameters and hard filters for nonmodel organisms, identical to Drott et al. (2020). Briefly: QD < 2.0 || FS > 60.0 || MQ < 40.0 || MQRankSum < −12.5 || ReadPosRankSum < −8.0 for single-nucleotide polymorphism (SNPs); and QD < 2.0 || FS > 200.0 || ReadPosRankSum < −20.0 for indels. Resulting data were filtered using VCFtools (v. 0.1.16) (Danecek et al. 2011) such that only biallelic sites that passed filters were retained. GATK is not designed to call SNPs from nanopore reads, so we manually compared SNP calls from PEPPER-Margin-DeepVariant (Shafin et al. 2021), Longshot (Edge and Bansal 2019), Nanocaller (Ahsan et al. 2021), and GATK to raw alignment files visualized in the Integrated Genomics Viewer (Robinson et al. 2011). GATK SNP calls were far better than calls from other programs and showed strong concordance between long- and short-read calls from the same isolate.

A total of 176 individuals and 1,268,021 sites were analyzed for genetic relationships. A distance matrix was inferred directly from the vcf file using plink (v. 1.90b6.21) (Purcell et al. 2007). To identify clones, the resulting distance matrix was converted into a histogram using R (Supplementary Fig. S1) and a cutoff value of 6,000 was selected based on a clear distribution of isolates with near-zero distance. Isolates that shared a distance less than the cutoff were considered clones and collapsed; one isolate per clonal group was randomly selected to be retained. A clone-corrected vcf file was created with 160 individuals and 1,268,021 sites. A neighbor-net network was created using SplitsTree (v. 6.1.16) (Huson and Bryant 2006) to visualize the genetic relationships among isolates. To understand how geographic isolation impacted genetic relationships, a Mantel test was performed using "gl.ibd" function of the "dartR" package in RStudio (Gruber et al. 2018) on both datasets. Geographic distance was calculated based on a single set of latitude and longitude coordinates at the center of each country of isolation obtained from https://developers.google.com/public-data/docs/canonical/countries_csv.

Trichothecene contamination

Trichothecene contamination in wheat flour samples from Ethiopia was determined using gas chromatography mass spectrometry (GC/MS) analysis as described in Mirocha et al. (1998) and Fuentes et al. (2005). Briefly, trichothecenes were extracted from wheat flour by taking 4 g from the 50-g bulk sample, mixing it with 16 ml of acetonitrile/water (84:16, vol/vol), and shaking the mixture on a rotary shaker for 1 h. A 4-ml extract was passed through a C18 and aluminum oxide (1:3, wt/wt) column. At room temperature (approximately 23°C), 1 ml of the filtrate was evaporated to dryness in a 1-dram vial under industrial grade nitrogen. After adding 100 μl of trimethylsilyl (TMS) reagent (TMSI/TMCS, 100/1), each vial was rotated to ensure complete contact between the filtrate and the reagent. The vials were placed on a shaker for 15 min. One milliliter of isooctane containing 0.5 μg/ml of mirex was added, followed by 1 ml of high-performance liquid chromatography water to quench the reaction. The vials were vortexed so that the milky isooctane layer became transparent. The upper layer of isooctane was transferred into a GC vial for GC/MS analysis (Shimadzu GCMS-QP2020, Shimadzu, Kyoto, Japan). The internal reference for GS/MS analysis was mirex (CAS number 2385-85-5), and pure DON, 3ADON, 15ADON, and NIV were used to construct the calibration curves for quantification.

Coinoculation assays

Based on preliminary species assignment from the ITS sequences, almost half of the 64 isolates were *Epicoccum* species. The large representation of *Epicoccum* species led us to hypothesize that there may be synergism between the *Epicoccum* and FGSC isolates. *F. graminearum* isolate PH-1 (isolated off corn from Michigan), *F. graminearum* isolate ET-2022-21 (from Ethiopia), and four *Epicoccum* species representatives (ET-2022-23, ET-2022-36, ET-2022-37-1, and ET-2022-56) (from Ethiopia) were selected for evaluations of virulence individually. Then, the isolates ET-2022-23 and ET-2022-56 were chosen as representative *E. ovisporum* and *E. sorghinum* isolates to do coinoculation assays with *F. graminearum* isolate ET-2022-21 in which the *Epicoccum*

isolate and the *F. graminearum* isolate were coinoculated at the same time or with 24 h between each inoculation. Two experiments were completed to establish the virulence of the isolates when inoculated alone and in coinoculations as described by Rafiei et al. (2025): a coleoptile assay and a leaf assay. Briefly, a coleoptile assay was performed in which coleoptiles from the wheat cv. Diskett, a spring wheat variety susceptible to *F. graminearum* as reported in other studies (Lennartsson 2024; Rafiei et al. 2025), were grown and inoculated, with each treatment being applied to 10 replicate coleoptiles. Disease symptoms were evaluated by measuring the longitudinal length of brown lesions on wheat coleoptiles' stems and leaves using a ruler at 7 days postinoculation (dpi).

Secondly, a leaf assay was performed as described by Browne and Cook (2004) with modifications based on (Perochon and Doohan 2016) and Rafiei et al. (2025) for coinoculations. Leaves from the wheat cv. Diskett were collected and inoculated, with each treatment being applied to a total of 12 replicate leaves. Disease development was assessed 4 dpi by measuring the lesion size on the leaf segments using Image J. The percent lesion area was calculated by dividing the lesion size by the leaf area and multiplying by 100. Leaf lesion area was transformed using an arcsine transformation to achieve homogeneity of variance.

Data analysis

Data analysis was performed using RStudio version 2024.06.05 "Chocolate Cosmos" (R version 4.4; Postit Team 2024). Data were analyzed with an analysis of variance. Post hoc Tukey means separation tests were conducted on treatment means. Graphs were created in RStudio using the package "ggplot2" (version 3.5.1; Wickham 2016).

Formal description of *Fusarium kistleri*

ET-2022-52, a novel species in the FGSC, is formally described based on morphology and phylogenetic distinctions as *Fusarium kistleri*. This isolate of *F. kistleri* was grown on carnation leaf agar (Fisher et al. 1982), synthetic nutrient-poor agar (SNA; Nirenberg 1976), oatmeal agar (OA; Crous et al. 2021), and PDA as described in Yilmaz et al. (2021). Morphological identification and characterization were conducted following protocols from Crous et al. (2021), Yilmaz et al. (2021), and Sandoval-Denis et al. (2025). Average colony morphology, growth rates, and pigmentation were determined by measuring the colony diameters on PDA (90-mm Petri dishes containing 25 ml of medium) after 7 days of incubation in the dark at 25°C (Yilmaz et al. 2021), using the color codes from Kornerup and Wanscher (1967). All measurements and images were captured using Nikon Eclipse Ni compound and SMZ18 dissecting microscopes (Nikon, Japan), equipped with a Nikon DS-Ri camera and the NIS-Elements BR imaging software. Up to 20 measurements were taken for conidia and other available morphological structures, with maximum, minimum, and average values calculated. Photographic plates were created using Affinity Photo v. 1.7.3 (Serif (Europe), Nottingham, U.K.).

Results

Causal pathogens associated with FHB symptoms on wheat

Based on the ITS-based species assignments, 45% of the 64 isolates were *Epicoccum* species and 19% were in the FGSC (Fig. 1). *Alternaria* and non-FGSC *Fusarium* species each represented 16% of the isolates. Disease severity rating was not predictive of the genera collected from the wheat heads ($P = 0.241$) (Supplementary Table S4). Given the relatively small number of FGSC species, we speculate many isolations reflect secondary infections and that *Fusarium* species were likely more ubiquitous than our sampling suggests. The diversity of isolated genera was not associated with geographic district ($P = 0.165$) or altitude ($P = 0.196$) of collection (Supplementary Fig. S2A and B). Similarly, species were not more common on a particular crop ($P = 0.457$) or variety ($P = 0.684$) (Supplementary Fig. S2C and D). A lack of significant association at the community level is not unexpected given our relatively small sample size. Obtaining FHB-related isolates from Ethiopia is challenging as no pipeline has been established because of the recent emergence of this disease. However, we suggest that our sampling is sufficient to capture many of the major players of the outbreak, if not to offer fine-scale resolution.

Epicoccum was the modal genus isolated from FHB-infected samples across Ethiopia with 29 isolates; 22 of these isolates were categorized as *E. sorghinum* using the ITS phylogenetic tree (Supplementary Fig. S3). Additionally, six of the *Epicoccum* isolates were *E. ovisporum* and one was *E. viticis* (Supplementary Fig. S3). Although ITS-based species assignments are tentative, the phylogeny we constructed does appear to differentiate these taxa from other closely related species.

Coinoculation assays

The large representation of *Epicoccum* and FGSC species raised questions about the potential of interspecies interactions. We used coleoptile and leaf assays to explore the nature of these interactions. First, six isolates and a mock treatment were inoculated alone to determine pathogenicity of the isolates under each assay. Coleoptiles inoculated with *F. graminearum* isolates (PH-1 and ET-2022-21) had greater disease severity compared with the mock treatment ($P \leq 0.001$) (Table 1). Whereas these two *F. graminearum* isolates did not cause different amounts of disease severity in coleoptile trials, the *F. graminearum* isolate from Ethiopia (ET-2022-21) caused significantly larger lesions (19.3% lesion area) than *F. graminearum* PH-1 (8.4% lesion area) on adult leaves ($P \leq 0.001$), emphasizing a need to further sample Ethiopian isolates to clarify whether isolates emerging there are more virulent in some circumstances. However, because all our *F. graminearum* isolates were clonal, we were unable to address this possibility here. *Epicoccum* caused very little disease severity in all plant assays, with no lesions developing on coleoptiles inoculated with the *Epicoccum* isolates (Table 1) and adult leaves only developing small lesions (<4% of leaf area) (data not shown). Based on these single inoculations, representative isolates of *E. ovisporum* and *E. sorghinum* were chosen to be used for coinoculations with the Ethiopian *F. graminearum* isolate.

Coinfection assays revealed that inoculation with *F. graminearum* (ET-2022-21) first and *Epicoccum* species 24 h later often caused greater lesions than those found in any other single or coinfection. Both coleoptile assays found that inoculation with *F. graminearum* followed by *E. sorghinum* resulted in significantly higher disease severity than *F. graminearum* alone ($P \leq 0.001$; Fig. 2A and B). However, this effect was not seen in adult leaves, where this coinfection caused significantly less disease severity than *F. graminearum* alone ($P = 0.007$) but still far more disease than *E. sorghinum* alone ($P \leq 0.001$; Fig. 3). Although the coinoculation of *F. graminearum* followed by *E. ovisporum* was not significantly different from *F. graminearum* alone in any of the three assays ($P \geq 0.197$), the coleoptile stem lesion assay trended toward higher disease severity in these conditions (Fig. 2A). Together, we conclude that when *Epicoccum*, particularly *E. sorghinum*, occurs as a secondary contaminant on wheat, it can have a small but sometimes significant impact on increasing disease progression.

Coinfections where *Epicoccum* species were concurrently inoculated with *F. graminearum* were not significantly different from inoculations with *F. graminearum* alone in any of the assays except for the adult leaf assay with *E. sorghinum* ($P = 0.046$; Fig. 3). In the latter assay, disease severity was significantly reduced (from 19 to 13%). However, all the concurrent coinoculations resulted in significantly higher disease severity than *Epicoccum* species alone ($P \leq 0.001$).

Coinfections where *Epicoccum* were inoculated first followed by *F. graminearum* resulted in significantly less disease severity than all other infections involving *F. graminearum* (including coinfections and individual infections, $P \leq 0.015$). In almost all leaf assays, these *Epicoccum*-first coinfections caused significantly more disease severity than *Epicoccum* alone, except for the *E. sorghinum* adult leaf assay and the *E. ovisporum* coleoptile leaf assay ($P = 0.999$ and $P = 0.945$, respectively).

Overall, the coinoculation assays demonstrate that the *F. graminearum* lineage evident in our sampling of Ethiopia can cause disease on wheat and may be more virulent than some strains like PH-1. Although different assays vary, we find that *Epicoccum* species can sometimes cause small synergistic increases in disease symptoms when they occur as a secondary infection. Conversely, establishment of *Epicoccum* first inhibits disease caused by *F. graminearum*. Although the assays performed here are designed for high throughput, allowing us to explore various aspects of the outbreak's etiology, they have been shown in other studies to significantly correlate with wheat-spike disease (Rafiei et al. 2025), suggesting that our results will translate to spike symptoms. Importantly, *Fusarium* infections in other parts of the plant, like those assayed here, are also biologically relevant, impacting yield and pathogen load in future years. The goal of this study was to begin to establish what is occurring in the 2022 Ethiopian outbreak. Future research should focus on further understanding the potential of interspecies interactions in the emergence of FHB in Ethiopia.

Quantify trichothecene contamination of wheat flour

Trichothecene contamination of wheat poses a serious threat to human and animal health. Of the 27 wheat flour samples, 15 had detectable levels of DON and 7 were at or above the limit of 1.0 ppm (Supplementary Table S5). Ten samples had detectable levels of NIV; one of these exceeded 1.0 ppm. However, eight of the samples (included in the abovementioned counts) had detectable levels of both DON and NIV. Trichothecene contamination of wheat flour was not affected by district ($P = 0.136$) of collection (Supplementary Table S6). There was no correlation between trichothecene contamination and FHB severity ratings ($P = 0.526$; Supplementary Table S6). However, there was a slight negative correlation between altitude and trichothecene contamination ($P = 0.049$; rho = –0.388; Spearman correlation test; Supplementary Table S6).

Determine trichothecene chemotype of FGSC isolates

Out of the 12 isolates that were classified as FGSC, 5 of the isolates were classified by genotyping as 15ADON, 3 as 3ADON, and 4 as NIV producers (Supplementary Fig. S4). Whole-genome sequencing clarified that chemotypes were largely siloed within species: all NIV isolates were *F. graminearum*, whereas all the 15ADON were *F. boothii*. The isolates classified as 3ADON were *F. aethiopicum* and ET-2022-52 (see species ID of this isolate below).

Determine the genetic relationship of the Ethiopian FGSC isolates to public data

The discovery of a new FGSC species, *F. aethiopicum*, in Ethiopia led O'Donnell et al. (2008) to suggest that the majority of species with the FGSC may have evolutionary origins in the Southern Hemisphere, raising questions about FGSC diversity in relatively understudied places like Ethiopia. To clarify the species identification of the 12 isolates that were classified as FGSC by ITS, we extracted gene sequences from corresponding genomes and compared them with the most comprehensive publicly available FGCC phylogenies, O'Donnell et al. (2008) and Laraba et al. (2021). Both trees provide evidence that four Ethiopian isolates are *F. graminearum*, five are *F. boothii*, and two are *F. aethiopicum*

Table 1. Mean lesion size (mm) ± standard error of infected wheat coleoptiles with different inoculation species 7 days postinoculation[z]

Inoculation	Species of isolate	Coleoptile stem lesion (mm)	Coleoptile leaf lesion (mm)
Mock	Mock	0.0 ± 0.0 b	0.0 ± 0.0 b
PH-1	*Fusarium graminearum*	9.3 ± 1.8 a	20.3 ± 4.2 a
ET-2022-21	*F. graminearum*	11.0 ± 1.4 a	24.5 ± 2.6 a
ET-2022-23	*Epicoccum sorghinum*	0.0 ± 0.0 b	0.0 ± 0.0 b
ET-2022-36	*E. sorghinum*	0.0 ± 0.0 b	0.0 ± 0.0 b
ET-2022-37-1	*E. ovisporum*	0.0 ± 0.0 b	0.0 ± 0.0 b
ET-2022-56	*E. ovisporum*	0.0 ± 0.0 b	0.0 ± 0.0 b

[z] Within each column, means ($n = 10$) followed by the same letter are not significantly different ($\alpha = 0.05$) as determined by the Tukey honestly significant difference post hoc test.

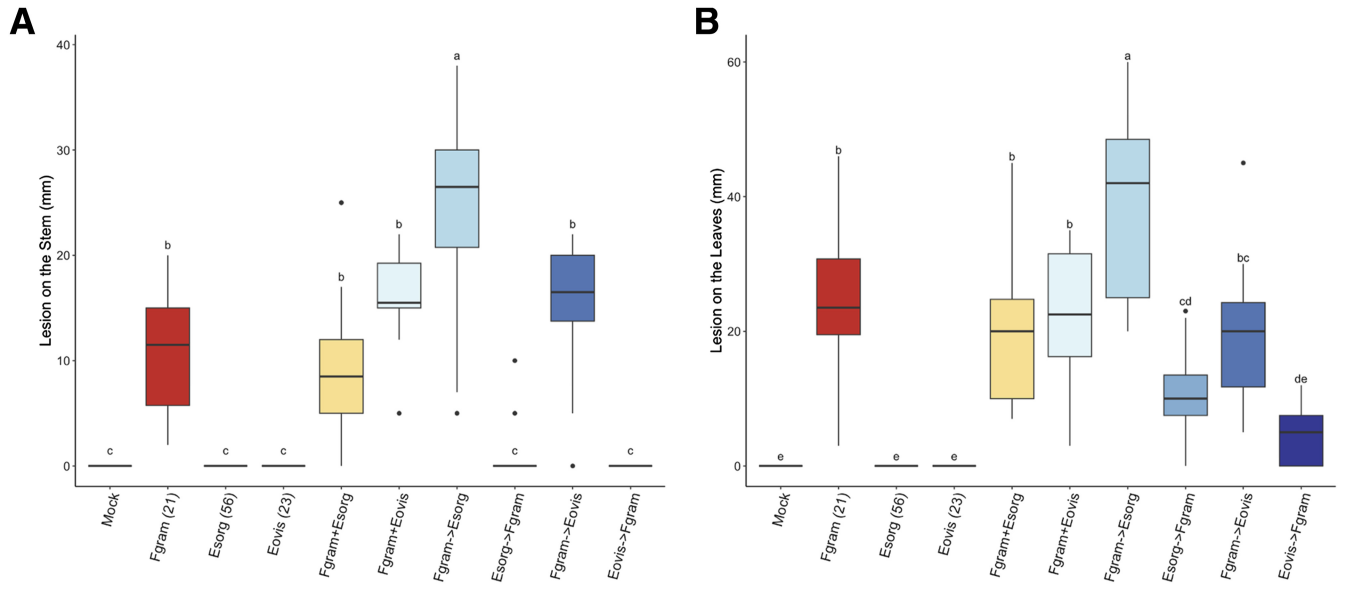

Fig. 2. Effect of inoculation treatments on coleoptile lesion size on the **A,** stem and **B,** leaves for *Fusarium graminearum* isolate ET-2022-21 (Fgram (21)), *Epicoccum sorghinum* isolate ET-2022-56 (Esorg (56)), and *E. ovisporum* isolate ET-2022-23 (Eovis (23)) alone and coinoculated. Coinoculations were made at the same time (indicated by a + symbol) or with one isolate inoculated 24 h prior to the other (indicated with an arrow representing the chronology from the first inoculated to second). Water was used as inoculant in the mock treatment. Treatment means ($n = 10$) followed by the same letter are not significantly different ($\alpha = 0.05$) as determined by the Tukey honestly significant difference post hoc test.

(Supplementary Fig. S5). However, one isolate (ET-2022-52) was not closely related to any known species. To further clarify the identity of the unresolved species, we downloaded 79 genomes and constructed a tree of the FGSC using 2,580 genes. This tree further corroborated the identity of all known species and confirmed that the isolate with no close relatives was a novel species (Fig. 4; Supplementary Figs. S6 and S7). Although ET-2022-52 was most closely related to *F. aethiopicum*, this relationship is consistent with ancient divergences between other FGSC species and is not compatible with intraspecific variation (Fig. 4). We have thus dubbed this novel species *Fusarium kistleri* and provide a formal species description below.

To better understand the relationship of known species found in Ethiopia, we performed a clone correction based on a distance matrix inferred directly from genome-wide SNP data (Supplementary Fig. S8). All four of the *F. graminearum* isolates belong to a single clonal lineage. Three out of the five *F. boothii* isolates (ET-2022-30, ET-2022-33, and ET-2022-35) are also clonal. Although high clonal fractions, especially of isolates sampled across different fields, could suggest an epidemic population structure, more sampling is needed to define population dynamics. Clone correction also collapsed the two datasets from isolates sequenced with both Nanopore and Illumina, respectively, suggesting both technologies yielded high-quality data.

F. graminearum isolates from Ethiopia are most closely related to *F. graminearum* isolates from Italy, Russia, and Germany in our neighbor-net network. However, the publicly available raw reads from Kulik et al. (2022) and Kelly and Ward (2018) only contained one *F. graminearum* isolate from Africa (SAMN16774551 from South Africa). When comparing across public data, we found that genetic differentiation could not be explained by physical distance for both non–clone-corrected and clone-corrected data (Mantel test, $P = 1$). We are hesitant to interpret these results given the geographic sampling bias of public data; more sampling in the Southern Hemisphere is needed to clarify the role of long-distance migration in the spreading of this pathogen.

Formal description of *Fusarium kistleri*

Taxonomy. The three phylogenetic analyses using a mix of nuclear ribosomal and protein-coding loci (detailed above) revealed that one isolate from Ethiopia was significantly distinct from other known *Fusarium* species within the *Fusarium sambucinum* species complex, particularly in FGSC. This isolate formed a unique clade with strong support in all maximum likelihood trees. We propose this new lineage as a new species, *Fusarium kistleri* sp. nov., which is described in this study along with its Latin binomial.

Fusarium kistleri Yilmaz, DeGenring, Gemechu, & Drott sp. nov. — MycoBank MB (MycoBank MB 859067); Figure 5.

Etymology. Latin, *kistleri*, refers to Dr. H. Corby Kistler in recognition of his outstanding career contributing to the *Fusarium* literature and to our understanding of FHB.

Typus. Ethiopia, Oromia region, from bread wheat cv. Kekeba (*Triticum aestivum*), collected by Ashenafi Gemechu on 29 October 2022, isolated by Ashenafi Gemechu and Karen Broz (holotype: PRU(M) 4624, designated here, dried specimen in metabolically inactive state, culture ex-type strain CBS 153210 = CMW 66453 =

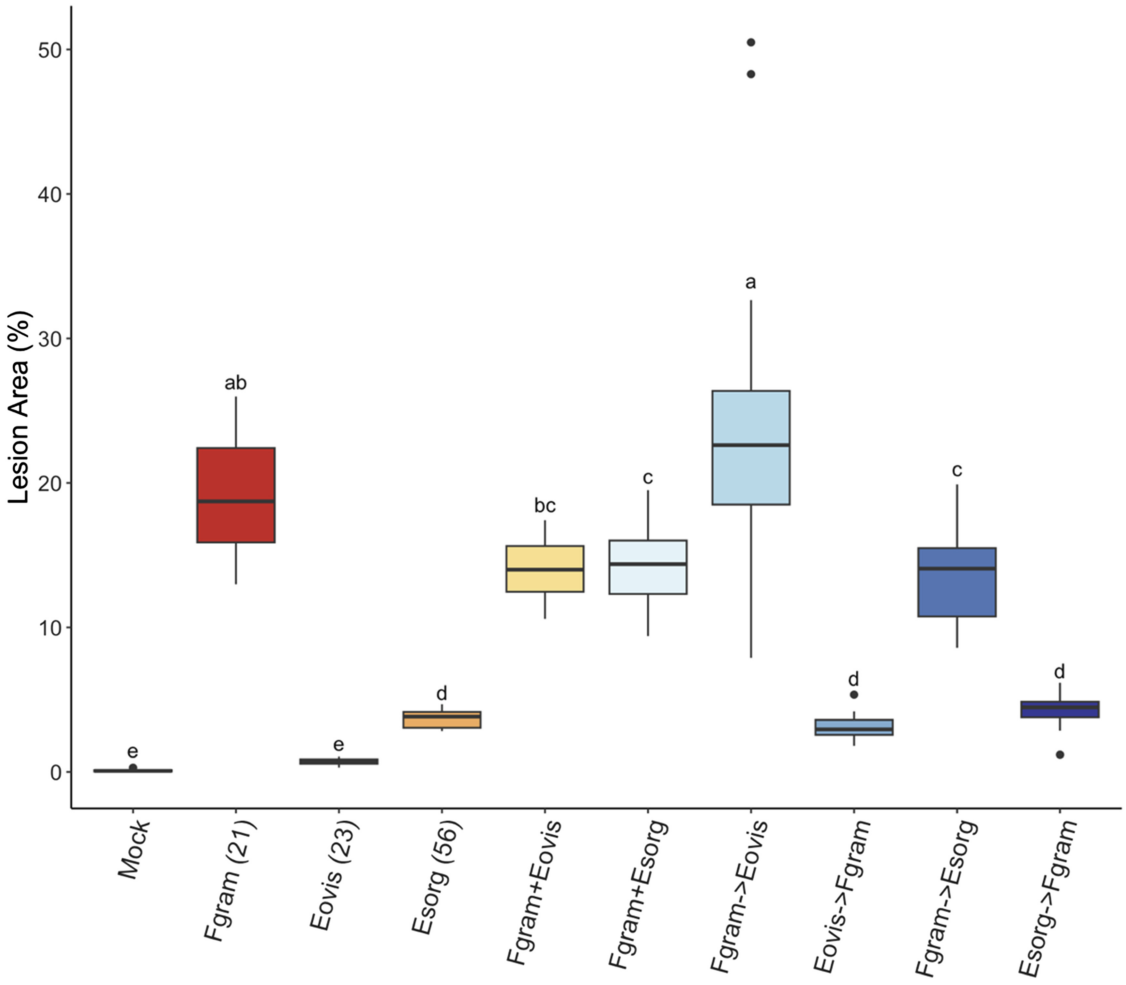

Fig. 3. Effect of inoculation treatments on adult leaf lesion area (%) for *Fusarium graminearum* isolate ET-2022-21 (Fgram (21)), *Epicoccum sorghinum* isolate ET-2022-56 (Esorg (56)), and *E. ovisporum* isolate ET-2022-23 (Eovis (23)) alone and coinoculated. Coinoculations were made at the same time (indicated by a + symbol) or with one isolate being inoculated 24 h prior to the other (indicated with an arrow representing the chronology from the first inoculated to second). Water was used as inoculant in the mock treatment. Treatment means ($n = 12$) followed by the same letter are not significantly different ($\alpha = 0.05$) as determined by the Tukey honestly significant difference post hoc test.

CMW-IA 7109 = CN229E8 = MTD-83 = ET-2022-52 = NRRL 64980).

Sporodochia were rare on aerial mycelium and agar, even after prolonged incubation (>1 month). When present, these structures appeared transparent to pale saffron or pale salmon in color. Sporodochial conidiophores were sparingly branched, 20 to 35 μm tall, monophialidic, subcylindrical to subulate, measuring (8–)10 to 15 × 3 to 6(–8) μm, smooth, thin-walled, with a short and flared apical collarette. Sporodochial conidia were predominantly 4- and 5-septate, typically falcate to gradually curved and asymmetric, with most conidia being wider above the median and lacking narrow apical beaks. Septation ranged from 3 to 5; 3-septate conidia: 22 to 30 × 4 to 6 μm (mean 26.7 × 5.2 μm); 4-septate conidia: (23–)27 to 38(–44) × 4.5 to 5.5(–6.3) μm (mean 31 × 5.3 μm); 5-septate conidia: 29 to 38(–41) × 4.5 to 5.5(–6) μm (mean 33.4 × 5.1 μm). Aerial conidiophores and (micro-) conidia were not observed. Chlamydospores were observed on both water agar and SNA under an alternating 12-h dark/12-h blacklight cycle. These structures were globose to

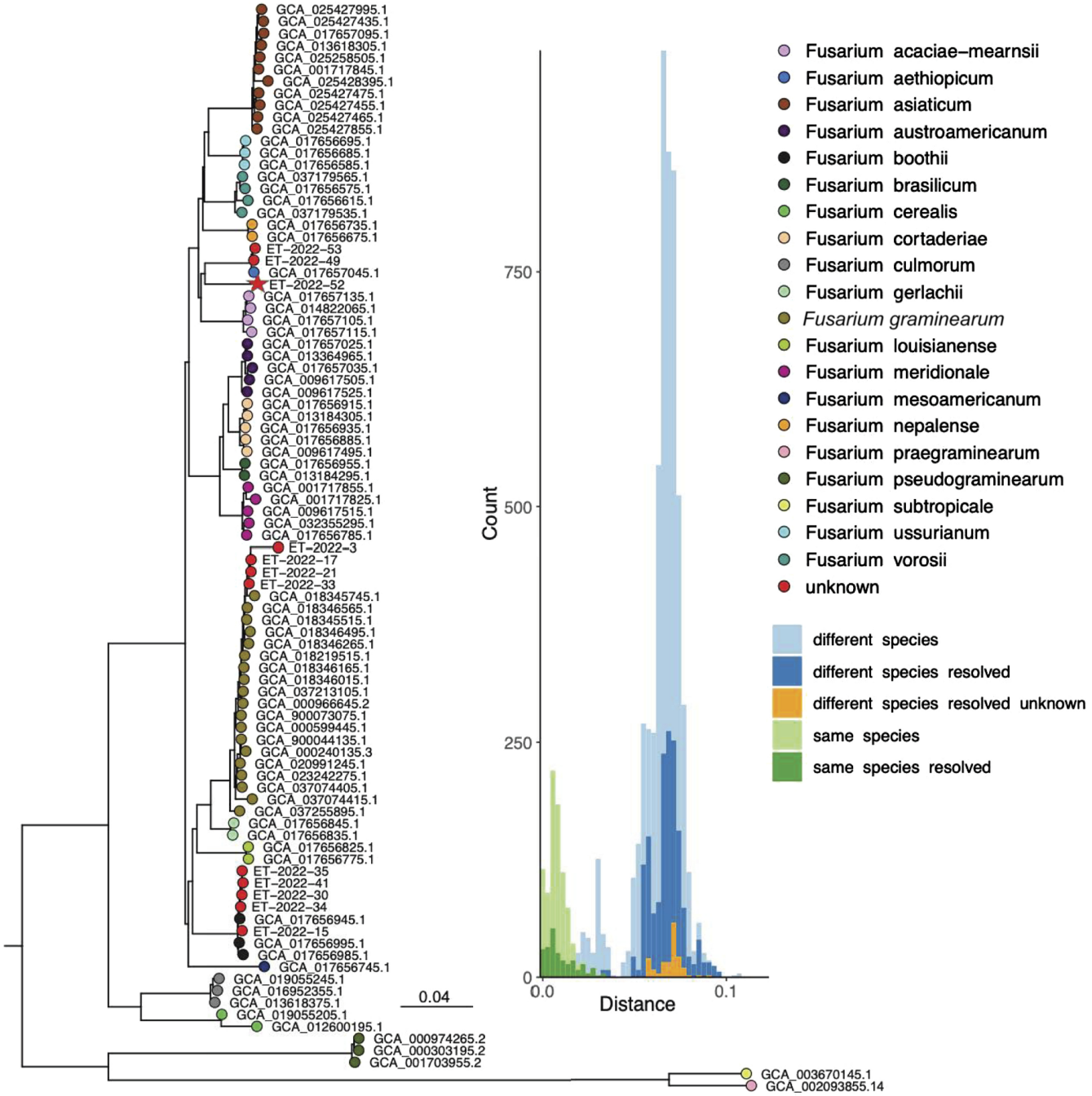

Fig. 4. The genetic distances within and between species support the discovery of a new species in the *Fusarium graminearum* species complex (FGSC). Genetic distances inferred from the maximum-likelihood tree (left) are depicted in a histogram (right) where distances between isolates of the same species are depicted in shades of green and distances between different species are colored in shades of blue. Lighter shades represent comparisons between species that were defined in other studies, whereas darker shades (also marked as "resolved") refer to comparisons with species identifications we inferred directly from the species tree. The distances depicted in orange are those between ET-2022-52 (marked with a star in the phylogeny), a novel species we describe in the main text as *Fusarium kistleri*, and all other isolates. Note that all our inferred species' identifications, including the novel species, fall squarely among genetic distances previously inferred as being between-species. The *x*-axis of the histogram has been truncated to depict only the closest genetic relationships. The phylogeny depicts the genetic relationships between 12 FGSC isolates from the 2022 Ethiopian outbreak (labels beginning with "ET" and indicated with red tips) and 79 publicly available genomes labeled with NCBI genomic accessions. Relationships were inferred using a partition model of 2,580 concatenated benchmarking single-copy orthologs (BUSCOs) that were present in all isolates. Ultrafast bootstrapping confirmed very strong support for nearly all branches, but to improve legibility, the bootstrapped tree has been relegated to the supplemental materials (Supplementary Fig. S6).

subglobose, smooth-walled, measuring (0.8–)1.05 to 1.10(–0.75) µm, hyaline, and occurring either solitary or in short chains. Perithecia were not observed. Characteristic odors were not detected.

Culture characteristics: Colonies on PDA at 25°C, grown in the dark, displayed an average radial growth rate of 7.5 to 9.5 mm/d, filling a 9-cm-diameter Petri dish after 7 days (Fig. 5). The colony surface was felty to woolly, rosy vinaceous to red, with white and pale luteous to luteous patches, and white at the center. Colonies were flat with abundant aerial mycelium, and the margins were regular. The reverse was straw to sulfur yellow at the center. Pigmentation intensified with prolonged incubation. On OA, colonies initially exhibited pure yellow to amber pigmentation, which later developed into rosy vinaceous to red. The colony surface was flat, cottony to woolly, with concentric rings of aerial mycelium and regular, filiform margins. The reverse was light scarlet with ochreous center.

Fusarium kistleri is resolved as a sister species to *F. aethiopicum* in phylogenetic analyses. Morphologically, it resembles other species within the Graminearum clade, including *F. asiaticum*, *F. graminearum*, *F. aethiopicum*, and *F. vorosii*. All these species produce asymmetric, slightly curved conidia that are predominantly 4- to 5-septate and measure 4 to 5 µm or more at their broadest point above the median (Aoki et al. 2012; O'Donnell et al. 2008; Sandoval-Denis et al. 2025). On OA, these species develop red and yellow pigmented, woolly colonies; however, pigmentation can vary depending on the conditions and the age of culture.

Although not mentioned in its protologue, Sandoval-Denis et al. (2025) reported that *F. aethiopicum* forms 0- to 3-septate, obovoid to ellipsoidal microconidia on aerial conidiophores. In contrast, *F. kistleri*, like *F. asiaticum*, *F. graminearum*, and *F. vorosii*, does not produce microconidia. When comparing the full range of sporodochial conidia, *F. kistleri* can be distinguished by its shorter conidia relative to *F. asiaticum*, *F. aethiopicum*, and *F. graminearum* (average lengths of 30 versus 38.8, 50.8, and 46.5 µm, respectively). Additionally, the conidia of *F. kistleri* are wider than those of *F. asiaticum* (5.2 versus 4.7 µm). Like its sister species *F. aethiopicum*, *F. kistleri* is known only from *Triticum* species in Ethiopia, based on a single isolate. In contrast, the morphologically similar *F. graminearum* has a cosmopolitan distribution and a broader host range (Farr et al. 2021; Sandoval-Denis et al. 2025).

Discussion

There have been few answers about the etiology of the 2022 FHB outbreak in Ethiopia. Although the intensification of wheat

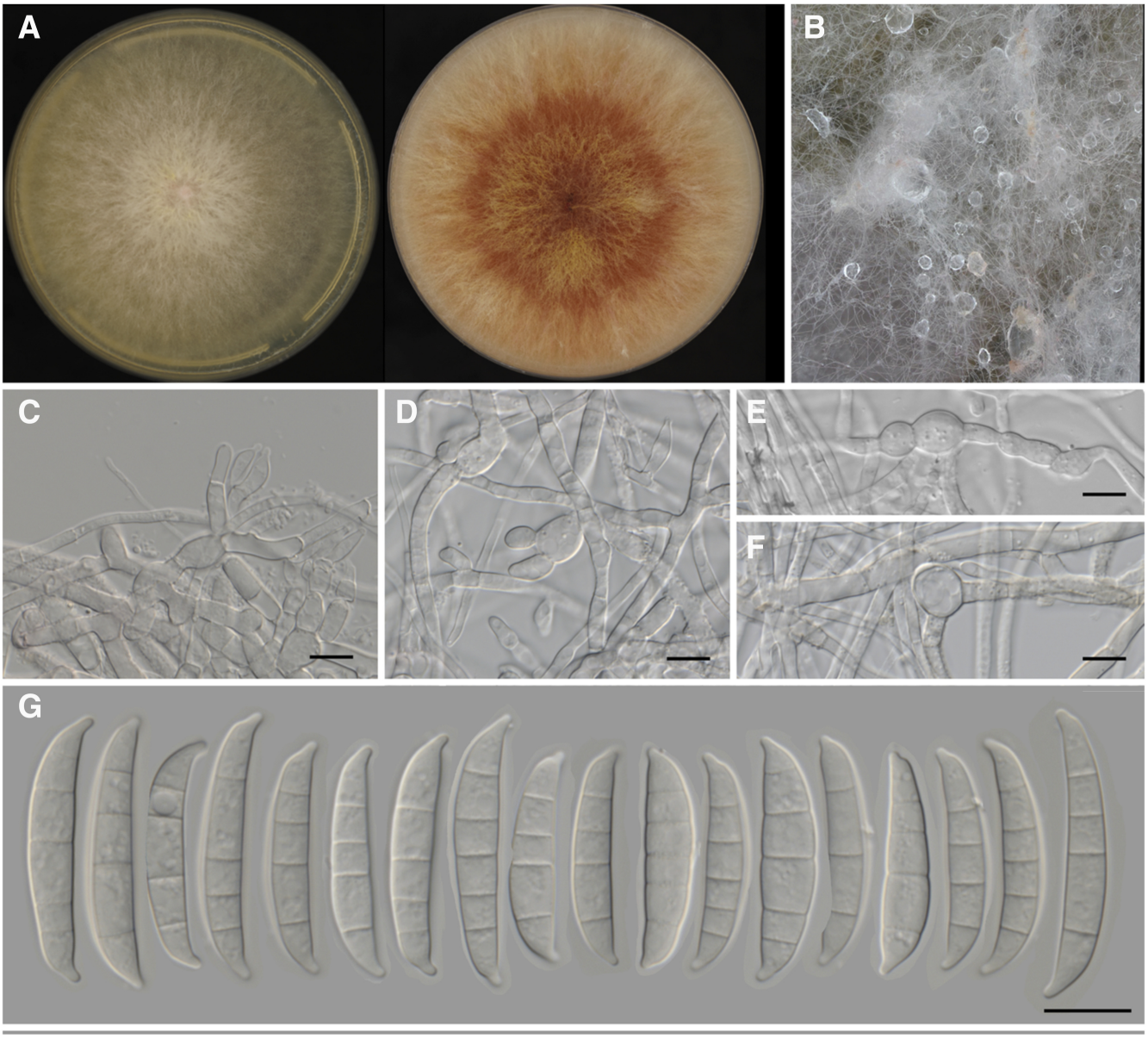

Fig. 5. Macroscopic and microscopic images of *Fusarium kistleri*. **A,** Colonies on potato dextrose agar (left) and oatmeal agar (right). **B,** Sporodochia and clusters of macroconidia. **C and D,** Conidiophores and conidiogenous cells. **E and F,** Chlamydospores. **G,** Macroconidia. Scale bars for C to G are 10 µm.

production in the country is likely a contributing factor, our results emphasize that this outbreak includes species that are rarely reported in other parts of the world. We found *F. boothii* in several wheat fields across the Amhara (North Shewa Zone) and Oromia (East Shewa Zone) regions. Although this species has been reported in South Africa, it mainly appears on corn and is rarely reported on wheat and in other parts of the world (Valverde-Bogantes et al. 2020). Environment-related species shifts have been reported in many countries and regions, for example, *F. culmorum* to *F. graminearum* in Europe (Ejaz et al. 2023; Infantino et al. 2023; Valverde-Bogantes et al. 2020). Even when accounting for recent shifts, the species found in the 2022 outbreak are still rare compared with any distribution reported in the literature. Indeed, to the best of our knowledge, there have been no reports of the *F. aethiopicum* lineage since the 2008 discovery (O'Donnell et al. 2008); all subsequent references have been general notes about species found in the FGSC. Our finding of *F. aethiopicum* in the 2022 outbreak shows that this species has persisted in Ethiopia over the 20 years since its discovery (as it was isolated from Ethiopian fields in 2003) and is contributing to FHB outbreaks. The new discovery of *F. kistleri* further emphasizes the unique species composition of this outbreak. Interestingly, this new species shares most recent ancestry with *F. aethiopicum*, suggesting some FHB-causing species may have ancient origins in this area. Even though commercial wheat production of modern varieties is historically rare in Eastern Africa, there is an ancient history of durum wheat cultivation in Ethiopia. Our results may suggest that FHB-causing lineages are ancient in Ethiopia, but it is unclear whether these lineages would have first associated with cultivated or native grasses as wild hosts have been observed to act as reservoirs in the United States (Lofgren et al. 2018).

The scarcity of literature on FGSC species that are rare in the United States and parts of Europe is not unique to the species found in Ethiopia. For example, *Fusarium nepalense*, discovered in Nepal, has also received little or no attention since it was first described (Sarver et al. 2011). Although this may reflect the limited agricultural impact of these pathogens, we suggest that studying these species presents a significant opportunity to contextualize the spread and pathogenicity of more common species and will help safeguard against future emergences. In the 2022 outbreak, rare *Fusarium* species threatened food safety and security through losses and mycotoxin contamination, with dangerous concentrations of trichothecenes found in 26% of grains. In the original article describing *F. aethiopicum*, a sample of only four isolates was used to confirm that this species has low to moderate virulence but accumulated significantly more DON than *F. graminearum* isolates (O'Donnell et al. 2008). Extensive profiling of *F. graminearum* isolates suggests that within species, FGSC isolates can have significant variation in agronomically important traits including virulence, toxin accumulation, and host range (Boutigny et al. 2011; Talas et al. 2012). These insights have enabled better disease prediction and control in countries like the United States (McMullen et al. 2012), but our results emphasize that there is a need to understand these traits for understudied FGSC species.

The pathogenicity of the FGSC often makes it the primary focus of FHB research, eclipsing other *Fusarium* species. In our study, nearly half of the *Fusarium* isolates (9 total) were not members of the FGSC. Of these non-FGSC isolates, 75% (6 total) were assigned to the *Fusarium incarnatum-equiseti* species complex (FIESC), and one isolate was assigned to the *Fusarium tricinctum* species complex (FTSC), based on phylogenetic relationships inferred from the ITS region. The remaining two non-FGSC isolates were members of the *Fusarium fujikuroi* species complex, which is not typically associated with FHB and may represent secondary infections (Supplementary Fig. S3). FIESC isolates are generally considered moderately virulent and often exhibit saprophytic tendencies, but these isolates can still produce mycotoxins (Desjardins 2006; O'Donnell et al. 2009). FTSC isolates are increasingly recognized as important pathogens of wheat and other cereals globally, with the ability to produce a wide array of toxic secondary metabolites (Laraba et al. 2022; Munkvold et al. 2021). Although these species complexes are not uncommon worldwide, their presence in symptomatic wheat heads and their association with high levels of disease severity further highlight the need for monitoring pathogen diversity and mycotoxin accumulation outside of the FGSC.

Historically, the United States, France, Canada, and Germany have been among the top 10 wheat-producing countries; thus, the scientific focus on *F. graminearum* may reflect not only issues in the countries driving FGSC research but also the most urgent problems facing regions of high wheat production. However, a recent analysis of global *F. graminearum* isolates suggests that international trade is likely contributing to the spread of this species (Broders et al., *personal communication*). Consistently, we find that Ethiopian *F. graminearum* isolates are most closely related to European isolates; although we are hesitant to directly interpret this result given limited public data from Africa, it raises questions about the importance of human-assisted migration. Dynamic shifts in FGSC species are common and predicted to increase with environmental shifts (Jung et al. 2022; Zhang et al. 2014), with some suggesting a direct linkage between the evolution of new FHB-causing lineages and these shifts (Nnadi and Carter 2021). In this study, we find high clonal fractions among *F. graminearum* and *F. boothii* isolates, with some clones isolated from multiple fields. Clonal expansions have been inferred for *F. graminearum* populations before: Kelly and Ward (2018) suggested that the low diversity of the NA2 population may reflect a clonal expansion after a population bottle neck, perhaps caused by a transcontinental introduction. Although we are hesitant to draw population-level conclusions from our small sample, the representative of the Ethiopian *F. graminearum* clonal lineage was indeed found to be more virulent in the leaf assay. The globalization of modern agriculture coupled with environmental shifts emphasizes the need to explore the virulence of diverse FGSC isolates under different conditions to help mitigate damage from emerging diseases and safeguard against future pathogens.

Although molecular work investigating virulence and DON has been dominated by *F. graminearum* grown in pure culture or in planta, many different FGSC species are often found in the same field (Boutigny et al. 2014), and a single species does not always make up the plurality of isolates (Audenaert et al. 2009). In the 2022 Ethiopian outbreak, we found that many different FGSC species and several different trichothecene chemotypes were present in the same field. Although trichothecene variants are thought to be associated with host specificity (Harris et al. 1999), it is not always clear what conditions or hosts favor which isolates. Furthermore, although total trichothecene content can contribute to threats to human health, there is little understanding of what implication multiple toxins in the same infection may have. In other systems, toxin combinations have sometimes been shown to have synergistic toxicities (Dowd 1988), and it has been suggested that one species can benefit from "cheating" dynamics from other isolates producing a different toxin (Drott et al. 2017). Historically, NIV producers have been more common in Asia, but in recent years, NIV has been increasingly documented in many places (Valverde-Bogantes et al. 2020). The presence of NIV, 15ADON, and 3ADON chemotypes in our relatively small sample of Ethiopia suggests that questions posed by the presence of mixed chemotypes in a single field are also relevant to emerging pathosystems.

Although many studies have documented the presence of different trichothecene chemotypes in the same field (Fulcher et al. 2019; Ward et al. 2008), interactions with mycotoxigenic species from other genera are less well understood. Coculturing different fungi together has been shown to initiate the production of otherwise "silent" secondary metabolite gene clusters, some of which encode known mycotoxins (Knowles et al. 2022). Here we found a surprising prevalence of *Epicoccum* species, particularly *E. sorghinum*, a species known to produce tenuazonic acid, a mycotoxin associated with ill-thrift in animals and hemorrhages in humans (Rychlik et al. 2016). *Epicoccum* species inhibited *Fusarium* growth when coinoculated, a result consistent with past efforts to use this genus, specifically *E. nigrum*, as a biocontrol for *F. graminearum* (Jensen et al. 2016;

Li et al. 2022). However, we found that when *E. sorghinum* arrives at a *Fusarium*-infected plant, it can have a small synergistic impact on disease symptom progression. *E. sorghinum* derives its name for sorghum, which is grown much more intensely in Ethiopia than in some other wheat-growing countries (i.e., correcting for geographic size, Sorghum production is approximately 4× higher in Ethiopia than the United States) (Foreign Agricultural Service 2023). The corn-wheat rotation in the United States is often invoked in helping explain the spread of FHB, with the suggestion that *F. graminearum* can overwinter on corn stubble (Leplat et al. 2013). There is even some suggestion that corn may select for specific chemotypes (Maier et al. 2006). Although our samples stem from regions of the Ethiopia where sorghum is not traditionally grown, our results highlight how little is known about potential interactions between cropping systems within a country.

Our findings emphasize that the 2022 FHB outbreak in Ethiopia is associated with globally rare species and mixed mycotoxins and may be impacted by intraspecific interactions that are not well understood. These factors represent challenges that are not confined to Ethiopia alone. The global research community has understandably focused on pathogen-host interactions that are relevant to their regions, yet this outbreak highlights the broader implications of FHB in a globalized agricultural landscape. Despite significant progress made by the Ethiopian Institute for Agricultural Research in managing plant disease in the country, FHB now poses challenges to the country's agriculture. The threat of FHB extends beyond national borders with recent evidence of human-assisted migration (Broders et al., *personal communication*), illustrating the global nature of this disease. As Ethiopia confronts FHB, there is still an opportunity for the global community to recognize the interconnectedness of agricultural economies and focus efforts to mitigate emerging diseases. The spread of the common pathogens and the emergence of new FHB-causing lineages poses a threat not only to food safety and food security but also to global food equity.

Literature Cited

Ahsan, M. U., Liu, Q., Fang, L., and Wang, K. 2021. NanoCaller for accurate detection of SNPs and indels in difficult-to-map regions from long-read sequencing by haplotype-aware deep neural networks. Genome Biol. 22:261.

Alisaac, E., and Mahlein, A.-K. 2023. Fusarium head blight on wheat: Biology, modern detection and diagnosis and integrated disease management. Toxins 15:192.

Allen-Sader, C., Thurston, W., Meyer, M., Nure, E., Bacha, N., Alemayehu, Y., Stutt, R. O. J. H., Safka, D., Craig, A. P., Derso, E., Burgin, L. E., Millington, S. C., Hort, M. C., Hodson, D. P., and Gilligan, C. A. 2019. An early warning system to predict and mitigate wheat rust diseases in Ethiopia. Environ. Res. Lett. 14:115004.

Amarasinghe, C., Sharanowski, B., and Fernando, W. G. D. 2019. Molecular phylogenetic relationships, trichothecene chemotype diversity and aggressiveness of strains in a global collection of *Fusarium graminearum* species. Toxins 11:263.

Amentae, T. K., Hamo, T. K., Gebresenbet, G., and Ljungberg, D. 2017. Exploring wheat value chain focusing on market performance, post-harvest loss, and supply chain management in Ethiopia: The case of Arsi to Finfinnee market chain. J. Agric. Sci. 9:22-42.

Anteneh, A., and Asrat, D. 2020. Wheat production and marketing in Ethiopia: Review study. Cogent Food Agric. 6:1778893.

Aoki, T., Ward, T. J., Kistler, H. C., and O'Donnell, K. 2012. Systematics, phylogeny and trichothecene mycotoxin potential of Fusarium head blight cereal pathogens. Mycotoxins 62:91-102.

Audenaert, K., Van Broeck, R., Bekaert, B., De Witte, F., Heremans, B., Messens, K., Höfte, M., and Haesaert, G. 2009. Fusarium head blight (FHB) in Flanders: Population diversity, inter-species associations and DON contamination in commercial winter wheat varieties. Eur. J. Plant Pathol. 125:445-458.

Ayelign, A., and De Saeger, S. 2020. Mycotoxins in Ethiopia: Current status, implications to food safety and mitigation strategies. Food Control 113:107163.

Bankevich, A., Nurk, S., Antipov, D., Gurevich, A. A., Dvorkin, M., Kulikov, A. S., Lesin, V. M., Nikolenko, S. I., Pham, S., Prjibelski, A. D., Pyshkin, A. V., Sirotkin, A. V., Vyahhi, N., Tesler, G., Alekseyev, M. A., and Pevzner, P. A. 2012. SPAdes: A new genome assembly algorithm and its applications to single-cell sequencing. J. Comput. Biol. 19:455-477.

Boutigny, A.-L., Ward, T. J., Ballois, N., Iancu, G., and Ioos, R. 2014. Diversity of the *Fusarium graminearum* species complex on French cereals. Eur. J. Plant Pathol. 138:133-148.

Boutigny, A.-L., Ward, T. J., Van Coller, G. J., Flett, B., Lamprecht, S. C., O'Donnell, K., and Viljoen, A. 2011. Analysis of the *Fusarium graminearum* species complex from wheat, barley and maize in South Africa provides evidence of species-specific differences in host preference. Fungal Genet. Biol. 48:914-920.

Browne, R. A., and Cooke, B. M. 2004. Development and evaluation of an *in vitro* detached leaf assay forc pre-screening resistance to Fusarium head blight in wheat. Eur. J. Plant Pathol. 110:91-102.

Bushnell, B. 2014. BBDuk: Adapter/quality trimming and filtering. https://sourceforge.net/projects/bbmap/

Capella-Gutiérrez, S., Silla-Martínez, J. M., and Gabaldón, T. 2009. trimAl: A tool for automated alignment trimming in large-scale phylogenetic analyses. Bioinformatics 25:1972-1973.

Correll, J. C., Klittich, C. J. R., and Leslie, J. F. 1987. Nitrate nonutilizing mutants of *Fusarium oxysporum* and their use in vegetative compatibility tests. Phytopathology 77:1640-1646.

Crous, P. W., Lombard, L., Sandoval-Denis, M., Seifert, K. A., Schroers, H.-J., Chaverri, P., Gené, J., Guarro, J., Hirooka, Y., Bensch, K., Kema, G. H. J., Lamprecht, S. C., Cai, L., Rossman, A. Y., Stadler, M., Summerbell, R. C., Taylor, J. W., Ploch, S., Visagie, C. M., Yilmaz, N., Frisvad, J. C., Abdel-Azeem, A. M., Abdollahzadeh, J., Abdolrasouli, A., Akulov, A., Alberts, J. F., Araújo, J. P. M., Ariyawansa, H. A., Bakhshi, M., Bendiksby, M., Ben Hadj Amor, A., Bezerra, J. D. P., Boekhout, T., Câmara, M. P. S., Carbia, M., Cardinali, G., Castañeda-Ruiz, R. F., Celis, A., Chaturvedi, V., Collemare, J., et al. 2021. *Fusarium*: More than a node or a foot-shaped basal cell. Stud. Mycol. 98:1-184.

Danecek, P., Auton, A., Abecasis, G., Albers, C. A., Banks, E., DePristo, M. A., Handsaker, R. E., Lunter, G., Marth, G. T., Sherry, S. T., McVean, G., Durbin, R., and 1000 Genomes Project Analysis Group. 2011. The variant call format and VCFtools. Bioinformatics 27:2156-2158.

Del Ponte, E. M., Moreira, G. M., Ward, T. J., O'Donnell, K., Nicolli, C. P., Machado, F. J., Duffeck, M. R., Alves, K. S., Tessmann, D. J., Waalwijk, C., van der Lee, T., Zhang, H., Chulze, S. N., Stenglein, S. A., Pan, D., Vero, S., Vaillancourt, L. J., Schmale, D. G., III, Esker, P. D., Moretti, A., Logrieco, A. F., Kistler, H. C., Bergstrom, G. C., Viljoen, A., Rose, L. J., van Coller, G. J., and Lee, T. 2022. *Fusarium graminearum* species complex: A bibliographic analysis and web-accessible database for global mapping of species and trichothecene toxin chemotypes. Phytopathology 112:741-751.

Demeke, M., and Di Marcantonia, F. 2013. Analysis of incentives and disincentives for wheat in Ethiopia. Technical Notes Series. MAFAP, FAO, Rome, Italy.

Desjardins, A. E. 2006. *Fusarium* Mycotoxins: Chemistry, Genetics, and Biology. American Phytopathological Society, St. Paul, MN, U.S.A.

Dowd, P. F. 1988. Synergism of aflatoxin B_1 toxicity with the co-occurring fungal metabolite kojic acid to two caterpillars. Entomol. Exp. Appl. 47:69-71.

Drott, M. T., Fessler, L. M., and Milgroom, M. G. 2019. Population subdivision and the frequency of aflatoxigenic isolates in *Aspergillus flavus* in the United States. Phytopathology 109:878-886.

Drott, M. T., Lazzaro, B. P., Brown, D. L., Carbone, I., and Milgroom, M. G. 2017. Balancing selection for aflatoxin in *Aspergillus flavus* is maintained through interference competition with, and fungivory by insects. Proc. R. Soc. B 284:20172408.

Drott, M. T., Satterlee, T. R., Skerker, J. M., Pfannenstiel, B. T., Glass, N. L., Keller, N. P., and Milgroom, M. G. 2020. The frequency of sex: Population genomics reveals differences in recombination and population structure of the aflatoxin-producing fungus *Aspergillus flavus*. mBio 11:e00963-20.

Edge, P., and Bansal, V. 2019. Longshot enables accurate variant calling in diploid genomes from single-molecule long read sequencing. Nat. Commun. 10:4660.

Ejaz, M. R., Jaoua, S., Ahmadi, M., and Shabani, F. 2023. An examination of how climate change could affect the future spread of *Fusarium* spp. around the world, using correlative models to model the changes. Environ. Technol. Innov. 31:103177.

Farr, D. F., Rossman, A. Y., and Castlebury, L. A. 2021. United States National Fungus Collections Fungus-Host Dataset. Ag Data Commons. https://doi.org/10.15482/USDA.ADC/1524414

Fisher, N. L., Burgess, L. W., Toussoun, T. A., and Nelson, P. E. 1982. Carnation leaves as a substrate and for preserving cultures of *Fusarium* species. Phytopathology 72:151-153.

Food and Agriculture Organization of the United Nations. 2021. Food Outlook: Biannual Report on Global Food Markets. FAO, Rome, Italy.

Foreign Agricultural Service (FAS). 2023. Production - Sorghum. Foreign Agricultural Service, Washington, DC, U.S.A.

Fuentes, R. G., Mickelson, H. R., Busch, R. H., Dill-Macky, R., Evans, C. K., Thompson, W. G., Wiersma, J. V., Xie, W., Dong, Y., and Anderson, J. A. 2005. Resource allocation and cultivar stability in breeding for Fusarium head blight resistance in spring wheat. Crop Sci. 45:1965-1972.

Fulcher, M. R., Winans, J. B., Quan, M., Oladipo, E. D., and Bergstrom, G. C. 2019. Population genetics of *Fusarium graminearum* at the interface of wheat and wild grass communities in New York. Phytopathology 109:2124-2131.

Gale, L. R., Harrison, S. A., Ward, T. J., O'Donnell, K., Milus, E. A., Gale, S. W., and Kistler, H. C. 2011. Nivalenol-type populations of *Fusarium graminearum* and *F. asiaticum* are prevalent on wheat in Southern Louisiana. Phytopathology 101:124-134.

Getahun, M., Fininsa, C., Mohammed, A., and Bekeko, Z. 2024. Integrated management of wheat (*Triticum aestivum* L.) Fusarium head blight and

deoxynivalenol contamination through host resistance and fungicide application in Ethiopia. J. Crop Sci. Biotechnol. 27:195-209.
Goswami, R. S., and Kistler, H. C. 2004. Heading for disaster: *Fusarium graminearum* on cereal crops. Mol. Plant Pathol. 5:515-525.
Gruber, B., Unmack, P. J., Berry, O. F., and Georges, A. 2018. dartr: An R package to facilitate analysis of SNP data generated from reduced representation genome sequencing. Mol. Ecol. Resour. 18:691-699.
Gurevich, A., Saveliev, V., Vyahhi, N., and Tesler, G. 2013. QUAST: Quality assessment tool for genome assemblies. Bioinformatics 29:1072-1075.
Haile, J. K., N'Diaye, A., Walkowiak, S., Nilsen, K. T., Clarke, J. M., Kutcher, H. R., Steiner, B., Buerstmayr, H., and Pozniak, C. J. 2019. Fusarium head blight in durum wheat: Recent status, breeding directions, and future research prospects. Phytopathology 109:1664-1675.
Hao, G., McCormick, S., Tiley, H., Gutiérrez, S., Yulfo-Soto, G., Vaughan, M. M., and Ward, T. J. 2023. NX trichothecenes are required for *Fusarium graminearum* infection of wheat. Mol. Plant-Microbe Interact. 36:294-304.
Harris, L. J., Desjardins, A. E., Plattner, R. D., Nicholson, P., Butler, G., Young, J. C., Weston, G., Proctor, R. H., and Hohn, T. M. 1999. Possible role of trichothecene mycotoxins in virulence of *Fusarium graminearum* on maize. Plant Dis. 83:954-960.
Huson, D. H., and Bryant, D. 2006. Application of phylogenetic networks in evolutionary studies. Mol. Biol. Evol. 23:254-267.
Infantino, A., Belocchi, A., Quaranta, F., Reverberi, M., Beccaccioli, M., Lombardi, D., and Vitale, M. 2023. Effects of climate change on the distribution of *Fusarium* spp. in Italy. Sci. Total Environ. 882:163640.
Jansen, C., von Wettstein, D., Schäfer, W., Kogel, K.-H., Felk, A., and Maier, F. J. 2005. Infection patterns in barley and wheat spikes inoculated with wild-type and trichodiene synthase gene disrupted *Fusarium graminearum*. Proc. Natl. Acad. Sci. U.S.A. 102:16892-16897.
Jensen, B. D., Knorr, K., and Nicolaisen, M. 2016. In vitro competition between *Fusarium graminearum* and *Epicoccum nigrum* on media and wheat grains. Eur. J. Plant Pathol. 146:657-670.
Jung, J.-Y., Kim, J.-H., Baek, M., Cho, C., Cho, J., Kim, J., Pavan, W., and Kim, K.-H. 2022. Adapting to the projected epidemics of Fusarium head blight of wheat in Korea under climate change scenarios. Front. Plant Sci. 13:1040752.
Kebede, M., Adugna, G., and Hundie, B. 2021. Status of Fusarium head blight on wheat fields in Southwestern Ethiopia. Ital. J. Mycol. 50:117-130.
Kelly, A. C., and Ward, T. J. 2018. Population genomics of *Fusarium graminearum* reveals signatures of divergent evolution within a major cereal pathogen. PLoS One 13:e0194616.
Knowles, S. L., Raja, H. A., Roberts, C. D., and Oberlies, N. H. 2022. Fungal–fungal co-culture: A primer for generating chemical diversity. Nat. Prod. Rep. 39:1557-1573.
Kolmogorov, M., Yuan, J., Lin, Y., and Pevzner, P. A. 2019. Assembly of long, error-prone reads using repeat graphs. Nat. Biotechnol. 37:540-546.
Kornerup, J. H., and Wanscher, A. 1967. Handbook of Colour, 2nd ed. Methuen & Company, London, U.K.
Kulik, T., Molcan, T., Fiedorowicz, G., van Diepeningen, A., Stakheev, A., Treder, K., Olszewski, J., Bilska, K., Beyer, M., Pasquali, M., and Stenglein, S. 2022. Whole-genome single nucleotide polymorphism analysis for typing the pandemic pathogen *Fusarium graminearum* sensu stricto. Front. Microbiol. 13:885978.
Laraba, I., Busman, M., Geiser, D. M., and O'Donnell, K. 2022. Phylogenetic diversity and mycotoxin potential of emergent phytopathogens within the *Fusarium tricinctum* species complex. Phytopathology 112:1284-1298.
Laraba, I., McCormick, S. P., Vaughan, M. M., Geiser, D. M., and O'Donnell, K. 2021. Phylogenetic diversity, trichothecene potential, and pathogenicity within *Fusarium sambucinum* species complex. PLoS One 16:e0245037.
Laraba, I., Ward, T. J., Cuperlovic-Culf, M., Azimi, H., Xi, P., McCormick, S. P., Hay, W. T., Hao, G., and Vaughan, M. M. 2023. Insights into the aggressiveness of the emerging North American population 3 (NA3) of *Fusarium graminearum*. Plant Dis. 107:2687-2700.
Lennartsson, E. 2024. Exploring Synergistic Effects of Soil Microorganisms in the Wheat Rhizosphere. Swedish University of Agricultural Sciences, Uppsala, Sweden.
Leplat, J., Friberg, H., Abid, M., and Steinberg, C. 2013. Survival of *Fusarium graminearum*, the causal agent of Fusarium head blight. A review. Agron. Sustain. Dev. 33:97-111.
Li, H. 2013. Aligning sequence reads, clone sequences and assembly contigs with BWA-MEM. arXiv preprint arXiv:1303.3997.
Li, H. 2018. Minimap2: Pairwise alignment for nucleotide sequences. Bioinformatics 34:3094-3100.
Li, H., Handsaker, B., Wysoker, A., Fennell, T., Ruan, J., Homer, N., Marth, G., Abecasis, G., Durbin, R., and 1000 Genome Project Data Processing Subgroup 2009. The sequence alignment/map format and SAMtools. Bioinformatics 25:2078-2079.
Li, T., Im, J., and Lee, J. 2022. Genetic diversity of *Epicoccum nigrum* and its effects on *Fusarium graminearum*. Mycobiology 50:457-466.
Liang, J. M., Xayamongkhon, H., Broz, K., Dong, Y., McCormick, S. P., Abramova, S., Ward, T. J., Ma, Z. H., and Kistler, H. C. 2014. Temporal dynamics and population genetic structure of *Fusarium graminearum* in the upper Midwestern United States. Fungal Genet. Biol. 73:83-92.
Lofgren, L. A., LeBlanc, N. R., Certano, A. K., Nachtigall, J., LaBine, K. M., Riddle, J., Broz, K., Dong, Y., Bethan, B., Kafer, C. W., and Kistler, H. C. 2018. *Fusarium graminearum*: Pathogen or endophyte of North American grasses? New Phytol. 217:1203-1212.
Maier, F. J., Miedaner, T., Hadeler, B., Felk, A., Salomon, S., Lemmens, M., Kassner, H., and Schäfer, W. 2006. Involvement of trichothecenes in fusarioses of wheat, barley and maize evaluated by gene disruption of the trichodiene synthase (Tri5) gene in three field isolates of different chemotype and virulence. Mol. Plant Pathol. 7:449-461.
McMullen, M., Bergstrom, G., De Wolf, E., Dill-Macky, R., Hershman, D., Shaner, G., and Van Sanford, D. 2012. A unified effort to fight an enemy of wheat and barley: Fusarium head blight. Plant Dis. 96:1712-1728.
Minh, B. Q., Schmidt, H. A., Chernomor, O., Schrempf, D., Woodhams, M. D., von Haeseler, A., and Lanfear, R. 2020. IQ-TREE 2: New models and efficient methods for phylogenetic inference in the genomic era. Mol. Biol. Evol. 37:1530-1534.
Minot, N., Warner, J., Lemma, S., Kasa, L., Gashaw, A., and Rashid, S. 2015. The Wheat Supply Chain in Ethiopia: Patterns, Trends, and Policy Options. Research for Ethiopia's Agricultural Policy (REAP), Washington, DC, U.S.A.
Mirocha, C. J., Kolaczkowski, E., Xie, W., Yu, H., and Jelen, H. 1998. Analysis of deoxynivalenol and its derivatives (batch and single kernel) using gas chromatography/mass spectrometry. J. Agric. Food Chem. 46:1414-1418.
Munkvold, G. P., Proctor, R. H., and Moretti, A. 2021. Mycotoxin production in *Fusarium* according to contemporary species concepts. Annu. Rev. Phytopathol. 59:373-402.
Negassa, A., Shiferaw, B., Koo, J., Sonder, K., Smale, M., Braun, H. J., Gbegbelegbe, S. D., Guo, Z., Hodson, D. P., Wood, S., Payne, T. S., and Abeyo, B. G. 2013. The Potential for Wheat Production in Africa: Analysis of Biophysical Suitability and Economic Profitability. CIMMYT, Texcoco, Mexico.
Nigus, M., Shimelis, H., Mathew, I., and Abady, S. 2022. Wheat production in the highlands of Eastern Ethiopia: Opportunities, challenges and coping strategies of rust diseases. Acta Agric. Scand. Sect. B 72:563-575.
Nirenberg, H. 1976. Untersuchungen über die morphologische und biologische Differenzierung in der Fusarium-Section Liseola. Mitteilungen der Biologischen Bundesanstalt für Land- und Forstwirtschaft. 169:1-117.
Nnadi, N. E., and Carter, D. A. 2021. Climate change and the emergence of fungal pathogens. PLoS Pathog. 17:e1009503.
O'Donnell, K., Kistler, H. C., Tacke, B. K., and Casper, H. H. 2000. Gene genealogies reveal global phylogeographic structure and reproductive isolation among lineages of *Fusarium graminearum*, the fungus causing wheat scab. Proc. Natl. Acad. Sci. U.S.A. 97:7905-7910.
O'Donnell, K., Sutton, D. A., Rinaldi, M. G., Gueidan, C., Crous, P. W., and Geiser, D. M. 2009. Novel multilocus sequence typing scheme reveals high genetic diversity of human pathogenic members of the *Fusarium incarnatum-F. equiseti* and *F. chlamydosporum* species complexes within the United States. J. Clin. Microbiol. 47:3851-3861.
O'Donnell, K., Ward, T. J., Aberra, D., Kistler, H. C., Aoki, T., Orwig, N., Kimura, M., Bjørnstad, Å., and Klemsdal, S. S. 2008. Multilocus genotyping and molecular phylogenetics resolve a novel head blight pathogen within the *Fusarium graminearum* species complex from Ethiopia. Fungal Genet. Biol. 45:1514-1522.
O'Donnell, K., Ward, T. J., Geiser, D. M., Kistler, H. C., and Aoki, T. 2004. Genealogical concordance between the mating type locus and seven other nuclear genes supports formal recognition of nine phylogenetically distinct species within the *Fusarium graminearum* clade. Fungal Genet. Biol. 41:600-623.
Perochon, A., and Doohan, F. M. 2016. Assessment of wheat resistance to *Fusarium graminearum* by automated image analysis of detached leaves assay. Bio-protocol 6:e2065.
Postit Team. 2024. RStudio: Integrated Development Environment for R. Postit Software. PBC, Boston, MA, U.S.A.
Purcell, S., Neale, B., Todd-Brown, K., Thomas, L., Ferreira, M. A. R., Bender, D., Maller, J., Sklar, P., de Bakker, P. I. W., Daly, M. J., and Sham, P. C. 2007. PLINK: A tool set for whole-genome association and population-based linkage analyses. Am. J. Hum. Genet. 81:559-575.
Quinlan, A. R., and Hall, I. M. 2010. BEDTools: A flexible suite of utilities for comparing genomic features. Bioinformatics 26:841-842.
Rafiei, V., DeGenring, L., Schwister, E. M., Elmore, J. M., Dubey, M., Karlsson, M., and Drott, M. T. 2025. Comparative analysis of distinct phenotyping methods for assessing wheat resistance and pathogen virulence among *Fusarium* species causing head blight disease. Plant Methods 21:85.
Reidy, J. 2024. Project Supports Ethiopian Wheat Production. World Grain, Kansas City, MO, U.S.A.
Robinson, J. T., Thorvaldsdóttir, H., Winckler, W., Guttman, M., Lander, E. S., Getz, G., and Mesirov, J. P. 2011. Integrative genomics viewer. Nat. Biotechnol. 29:24-26.
Rychlik, M., Lepper, H., Weidner, C., and Asam, S. 2016. Risk evaluation of the *Alternaria* mycotoxin tenuazonic acid in foods for adults and infants and subsequent risk management. Food Control 68:181-185.
Sandoval-Denis, M., Costa, M. M., Broders, K., Becker, Y., Maier, W., Yurkov, A., Kermode, A., Buddie, A. G., Ryan, M. J., Schumacher, R. K., Groenewald, J. Z., and Crous, P. W. 2025. An integrative re-evaluation of the *Fusarium sambucinum* species complex. Stud. Mycol. 110:1-110.

Sarver, B. A. J., Ward, T. J., Gale, L. R., Broz, K., Corby Kistler, H., Aoki, T., Nicholson, P., Carter, J., and O'Donnell, K. 2011. Novel Fusarium head blight pathogens from Nepal and Louisiana revealed by multilocus genealogical concordance. Fungal Genet. Biol. 48:1096-1107.

Schmale, D. G., III, and Bergstrom, G. C. 2003. Fusarium Head Blight (FHB) or Scab. The Plant Health Instructor, St. Paul, MN, U.S.A.

Schmeitzl, C., Warth, B., Fruhmann, P., Michlmayr, H., Malachová, A., Berthiller, F., Schuhmacher, R., Krska, R., and Adam, G. 2015. The metabolic fate of deoxynivalenol and its acetylated derivatives in a wheat suspension culture: Identification and detection of DON-15-*O*-glucoside, 15-acetyl-DON-3-*O*-glucoside and 15-acetyl-DON-3-sulfate. Toxins 7:3112-3126.

Shafin, K., Pesout, T., Chang, P.-C., Nattestad, M., Kolesnikov, A., Goel, S., Baid, G., Kolmogorov, M., Eizenga, J. M., Miga, K. H., Carnevali, P., Jain, M., Carroll, A., and Paten, B. 2021. Haplotype-aware variant calling with PEPPER-Margin-DeepVariant enables high accuracy in nanopore long-reads. Nat. Methods 18:1322-1332.

Shiferaw, B., Smale, M., Braun, H.-J., Duveiller, E., Reynolds, M., and Muricho, G. 2013. Crops that feed the world 10. Past successes and future challenges to the role played by wheat in global food security. Food Secur. 5:291-317.

Simão, F. A., Waterhouse, R. M., Ioannidis, P., Kriventseva, E. V., and Zdobnov, E. M. 2015. BUSCO: Assessing genome assembly and annotation completeness with single-copy orthologs. Bioinformatics 31:3210-3212.

Starkey, D. E., Ward, T. J., Aoki, T., Gale, L. R., Kistler, H. C., Geiser, D. M., Suga, H., Tóth, B., Varga, J., and O'Donnell, K. 2007. Global molecular surveillance reveals novel Fusarium head blight species and trichothecene toxin diversity. Fungal Genet. Biol. 44:1191-1204.

Tadesse, W., Bishaw, Z., and Assefa, S. 2019. Wheat production and breeding in Sub-Saharan Africa: Challenges and opportunities in the face of climate change. Int. J. Clim. Change Strateg. Manage. 11:696-715.

Tadesse, W., Zegeye, H., Debele, T., Kassa, D., Shiferaw, W., Solomo, T., Negash, T., Geleta, N., Bishaw, Z., and Assefa, S. 2022. Wheat production and breeding in Ethiopia: Retrospect and prospects. Crop Breed. Genet. Genom. 4:e220003.

Talas, F., Kalih, R., and Miedaner, T. 2012. Within-field variation of *Fusarium graminearum* isolates for aggressiveness and deoxynivalenol production in wheat head blight. Phytopathology 102:128-134.

Valverde-Bogantes, E., Bianchini, A., Herr, J. R., Rose, D. J., Wegulo, S. N., and Hallen-Adams, H. E. 2020. Recent population changes of Fusarium head blight pathogens: Drivers and implications. Can. J. Plant Pathol. 42:315-329.

Van der Auwera, G. A., and O'Connor, B. D. 2020. Genomics in the Cloud: Using Docker, GATK, and WDL in Terra. O'Reilly Media, Sebastopol, CA, U.S.A.

Varga, E., Wiesenberger, G., Hametner, C., Ward, T. J., Dong, Y., Schöfbeck, D., McCormick, S., Broz, K., Stückler, R., Schuhmacher, R., Krska, R., Kistler, H. C., Berthiller, F., and Adam, G. 2015. New tricks of an old enemy: Isolates of *Fusarium graminearum* produce a type A trichothecene mycotoxin. Environ. Microbiol. 17:2588-2600.

Ward, T. J., Bielawski, J. P., Kistler, H. C., Sullivan, E., and O'Donnell, K. 2002. Ancestral polymorphism and adaptive evolution in the trichothecene mycotoxin gene cluster of phytopathogenic *Fusarium*. Proc. Natl. Acad. Sci. U.S.A. 99:9278-9283.

Ward, T. J., Clear, R. M., Rooney, A. P., O'Donnell, K., Gaba, D., Patrick, S., Starkey, D. E., Gilbert, J., Geiser, D. M., and Nowicki, T. W. 2008. An adaptive evolutionary shift in Fusarium head blight pathogen populations is driving the rapid spread of more toxigenic *Fusarium graminearum* in North America. Fungal Genet. Biol. 45:473-484.

White, T. J., Bruns, T. D., Lee, S. B., and Taylor, J. W. 1990. Amplification and direct sequencing of fungal ribosomal RNA genes for phylogenetics. Pages 315-322 in: PCR Protocols: A Guide to Methods and Applications. M. A. Innis, D. H. Gelfand, J. J. Sninsky, and T. J. White, eds. Academic Press, San Diego, CA.

Wickham, H. 2016. ggplot2: Elegant Graphics for Data Analysis. Springer-Verlag, New York, NY, U.S.A.

Xu, M., Wang, Q., Wang, G., Zhang, X., Liu, H., and Jiang, C. 2022. Combatting Fusarium head blight: Advances in molecular interactions between *Fusarium graminearum* and wheat. Phytopathol. Res. 4:37.

Yilmaz, N., Sandoval-Denis, M., Lombard, L., Visagie, C. M., Wingfield, B. D., and Crous, P. W. 2021. Redefining species limits in the *Fusarium fujikuroi* species complex. Persoonia 46:129-162.

Zhang, X., Halder, J., White, R. P., Hughes, D. J., Ye, Z., Wang, C., Xu, R., Gan, B., and Fitt, B. D. L. 2014. Climate change increases risk of Fusarium ear blight on wheat in central China. Ann. Appl. Biol. 164:384-395.

Zhang, Z., Schwartz, S., Wagner, L., and Miller, W. 2000. A greedy algorithm for aligning DNA sequences. J. Comput. Biol. 7:203-214.